Journal of Sound and Vibration (2002) **249**(1), 206–212
doi:10.1006/jsvi.2001.3684, available online at http://www.idealibrary.com on IDEAL®

SOUND TRANSMISSION THROUGH A RIB-STIFFENED PLATE: COMPARISONS OF A LIGHT-FLUID APPROXIMATION WITH EXPERIMENTAL RESULTS

C. MAURY† AND P.-O. MATTEI

Laboratoire de Mécanique et d'Acoustique, 31 *chemin Joseph Aiguier*, 13402 *Marseille cedex* 20, *France*

(*Received* 21 *February* 2000, *and in final form* 26 *March* 2001)

1. INTRODUCTION

Interest in stiffened-plate constructions has been widespread recently in aerospace, marine and engineering structures: their vibratory response can be greatly modified by small weight added to the hull. Several methods have been presented for the dynamic analysis of such structures. Analytical methods easily account for the fluid-loading coupling but they are restrained either to a great number of equally spaced stiffeners [1] or to ribs with an infinite mechanical impedance [2]. Semi-analytical [3, 4] and finite-element [5] modellings are mostly based on a weak (energetic) formulation of the *in vacuo* problem. First, the analysis has been simplified by applying the so-called orthotropic equivalent plate theory [6], only valid when the mechanical wavelengths are greater than the stiffeners spacing; a more accurate and robust method is the discrete model in which the system is divided into subelements: the stiffeners are therefore considered as beams exerting efforts on the plate [7].

The structural analysis used in this paper follows this method. Moreover, the vibro-acoustic response of the system fluid/structure is approximated under the assumption that the fluid loading is a small perturbation with respect to the *in vacuo* problem since the surrounding fluid is a gas. A more thorough investigation of perturbation methods for predicting the sound radiated by a vibrating plate in a light fluid has been examined in two recent references [8, 9]. This paper applies this approximation to the case of a baffled plate stiffened by ribs.

2. THEORETICAL ANALYSIS

Consider the thin elastic plate shown in Figure 1, occupying the domain Σ of the $z = 0$ plane and stiffened by two eccentric T-section ribs parallel to the y-axis. The rectangular baffled plate, with thickness h, is clamped along its boundary $\partial\Sigma$ with normal unit vector $\mathbf{n}$. It separates two half-spaces containing a perfect gas with density μ_0.

2.1. THE RIB-STIFFENED PLATE MODEL

The thin beam approximation assumed for stiffeners with a thickness/length ratio of 2%, as used in the experiment, is a very crude approximation. However, as shown in

†Present address: Institute of Sound and Vibration Research, University of Southampton, Southampton SO17 1BJ, England.

0022-460X/02/010206 + 07 $35.00/0

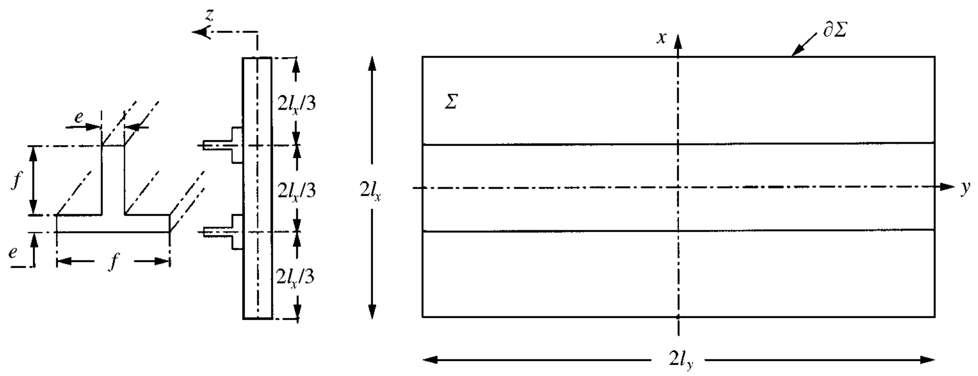

Figure 1. A plate stiffened by two T-ribs.

TABLE 1

Comparison between the measured and computed eigenfrequencies of the stiffeners

Eigenfrequencies (real part) of the stiffeners (Hz)		
Measured	Computed	Relative error (%)
21·5	21·4	0·5
134·2	134·3	0·1
373	376	0·8
721	736	2
1168	1216	4
1711	1816	6
2331	2597	10
3012	3374	11

Table 1, it can be seen that this approximation remains valid up to the fourth natural frequency of the beam (721 Hz) with an error less than 2%. Above this frequency, it has been noted that this approximation provides erroneous results and so the study is limited to the low-frequency domain.

Since the stiffeners are attached on one side of the plate, the flexural and membrane action of the plate are *a priori* coupled. However, as shown by Petyt [10], the in-plane contribution has little effect on the first few natural frequencies of a stiffened plate. Thus, for the low-frequency range considered in this paper (up to about 30 natural modes), neglecting the in-plane deformations is a reasonable approximation.

2.2. GOVERNING EQUATIONS FOR THE RESPONSE OF A BAFFLED PLATE STIFFENED BY TWO RIBS

Let $P_0(M)$ be the sound pressure generated by an acoustic source distribution ($e^{-i\omega t}$) in the $z < 0$ half-space and $w(M)$, the plate deflection, positive in the $z > 0$ direction. Let $\mathcal{G}_w$ be the Green function which satisfies the Helmholtz equation in the fluid medium with a Neumann boundary condition on $z = 0$.

Using the Green representation of the acoustic pressure [8], the initial boundary-value problem is replaced by an integro-differential equation which governs the plate displacement:

$$(D\Delta^2 - \mu\omega^2)\, w(M) + 2\omega^2\mu_0 \int_\Sigma w(M')\mathscr{G}_\omega(M, M')\, \mathrm{d}\sigma(M')$$

$$= \left(P_0 - \sum_{j=1}^{2} F_j\right)(M),\ M \in \Sigma,$$

$$F_j(M) = \left(E_j I_j^x \frac{\mathrm{d}^4}{\mathrm{d}y^4} - \rho_j A_j \omega^2\right) w_{R_j}(y)\delta_{x_j}(x), \qquad j = 1, 2, \quad M \in \Sigma,$$

$$w_{R_j}(y) = w(x_j, y), \qquad j = 1, 2, \quad y \in [-l_y, l_y],$$

$$w(M) = \partial_{\vec{n}} w(M) = 0, \quad M \in \partial\Sigma,$$

where D is the bending rigidity of the plate and μ its mass per unit area; F_j is the normal force exerted on the jth stiffener by the plate along the junction line; E_j and $\rho_j A_j$ are Young's modulus and the mass per unit length of each stiffener; and I_j^x is the second moment of area of each rib cross-section about the axis in the middle surface of the plate.

2.3. THE PERTURBATION METHOD APPLIED TO THE MODAL ANALYSIS OF THE FLUID-LOADED STRUCTURE

The plate displacement w is expanded into a series of eigenmodes W_n of the fluid-loaded structure. The eigenmodes and their corresponding eigenvalues Λ_n are sought as a series of the small parameter $\varepsilon(= 2\mu_0/\mu)$:

$$W_n = W_n^0 + \varepsilon W_n^1 + \cdots, \qquad \Lambda_n = \Lambda_n^0 + \varepsilon \Lambda_n^1 + \cdots.$$

These expansions are then introduced into the eigenmodes series representation of the plate displacement [8]. Hence, w is approximated to the first order by

$$w(M) \simeq \sum_{n=1}^{N} \left\{ \frac{W_n^0(M)}{(\Lambda_n - \mu\omega^2)} \left[\frac{\langle S, W_n^{0*} \rangle}{N_n} + \varepsilon \sum_{q=1, q\neq n}^{Q} \frac{1}{\Lambda_n - \Lambda_q} \left(\frac{\Lambda_n}{(\Lambda_n - \mu\omega^2)} - \frac{\Lambda_q}{(\Lambda_q - \mu\omega^2)} \right) \frac{\beta_\omega(W_q^0, W_n^{0*}) \langle S, W_q^{0*} \rangle}{N_n N_q} \right] \right\}, \tag{1}$$

where N_n is the norm associated to the orthogonality relationship between the *in vacuo* eigenmodes W_n^0 of the stiffened plate. These are computed as a series of functions of Legendre polynomials satisfying regularity conditions as well as boundary conditions on $\partial\Sigma$. The bilinear forms in equation (1) are defined by

$$\langle u, v \rangle = \int_\Sigma u(M) v^*(M)\, \mathrm{d}M, \qquad \beta_\omega(u, v) = \int_\Sigma \int_\Sigma u(M)\mathscr{G}_\omega(M, M') v^*(M')\, \mathrm{d}M\, \mathrm{d}M'.$$

A specific integration algorithm is used to rapidly give an accurate estimation of the coupling term β_ω which is the most time consuming. The numbers N and Q of the eigenmodes that are accounted for is determined by the number of those which are necessary for an accurate representation of the excitation P_0.

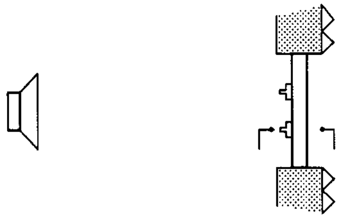

Figure 2. Experimental set-up for sound transmission measurements.

3. COMPARISONS BETWEEN NUMERICAL PREDICTIONS AND EXPERIMENTAL RESULTS

In order to validate this approach, an experiment has been carried out in the twin anechoic rooms of the Laboratoire de Mécanique et d'Acoustique. A large anechoic room is connected to a smaller semi-anechoic room by an aperture in which the plate is clamped. The wall between the two rooms is an almost perfectly rigid plane on the semi-anechoic side and covered with glass-wool wedges on the anechoic side (the baffle is almost perfectly absorbant). As shown in Figure 2, the acoustic sound source is located in the semi-anechoic room.

While the experimental conditions are somewhat different from the theoretical model, which assumes a perfectly rigid baffle on both sides of the plate, it can easily be seen that the transmitted sound field very close to the plate is not influenced too much by the reflecting properties of the baffle. Moreover, the uncertainties of the mechanical properties of both the plate and the stiffeners, the non-perfect clamping of the plate or the non-perfect fixing of the stiffeners, bolted on the plate, induce more significant errors.

The experimental plate is made of stainless steel with dimensions $1\ \mathrm{m} \times 1\cdot 54\ \mathrm{m}$. Its thickness has been measured at more than 20 points and a mean value of $1\cdot 9$ mm has been obtained. The mean value of the mass per unit area could then be deduced and is given by $\mu = 15\cdot 6\ \mathrm{kg/m^2}$. The rigidity of the plate was obtained experimentally by the following procedure. A flat circular plate (10 cm radius) was made in the same material. The first eigenfrequencies of the free plate were measured and the rigidity adjusted to get the best fit with the experimental ones. This leads to $D = 122$ Nm; the Poissons' ratio is given by $\nu = 0\cdot 33$. The mechanical characteristics of the stiffeners, made of aluminium, were estimated in the same way. A 1-m-long stiffener built in the same material was clamped at one end while the other end rested free. The comparison between the first measured and computed eigenfrequencies lead to a fitted Young's modulus $E = 67\cdot 6$ GPa (see Table 1). The density of the stiffeners material is given by $\rho = 2600\ \mathrm{kg/m^3}$.

In Table 2, a comparison between the experimental and measured eigenfrequencies of the fluid-loaded clamped stiffened plate is presented. As can be seen, the results agree within a few per cent. It is to be noticed that for a stiffened plate, there is a better agreement between the experiment and the theory than for a plate without stiffeners: the stiffeners smooth the inhomogeneity of the plate (made of industrial material).

A transfer function between two microphones (see Figure 2) has been measured and computed in terms of the excitation frequency. The results are presented in Figures 3 and 4. For the prediction, a structural damping has been accounted for by considering an imaginary part for Young's modulus of the materials. The usual values can be found in reference [11]. Although some discrepancies can be noticed for the peak levels between the experimental and the predicted data in Figure 3, the results presented here validate the

TABLE 2

Comparison between the measured and computed eigenfrequencies of the rib-stiffened plate

Eigenfrequencies (*real part*) *of the rib stiffened* (Hz)			
Measured	Computed	Measured	Computed
13·7	14·1	90	90·1
26	27·4	99	100·2
34	35·2	107	109·3
46	45·7	113	116·2
47	47·5	118	121·1
57	56·2	129	127·5
63	62·3	134	131·7
72	75·2	146	143·6
78	78·2	148	148·4
81	81·1	150	154·5
87	88·3	158	156·6

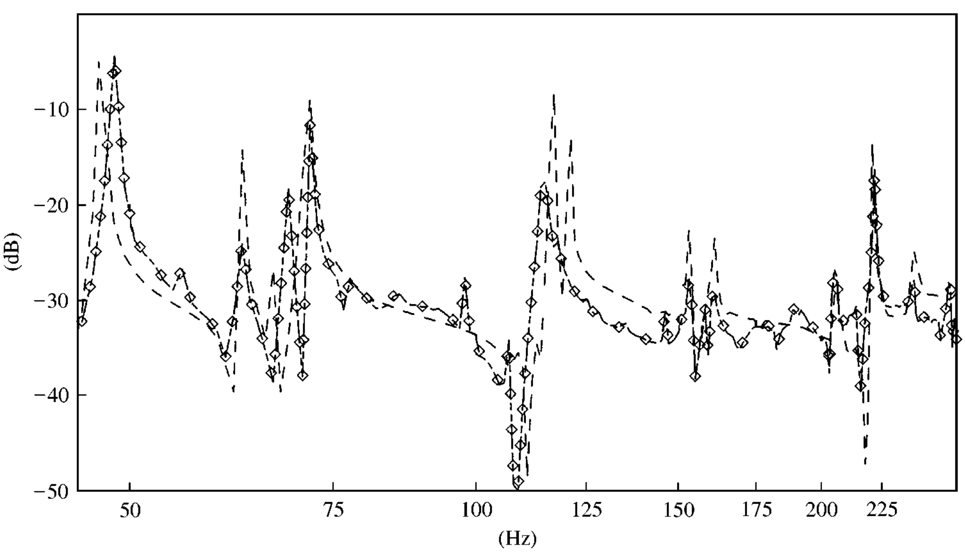

Figure 3. Comparison between the measured transfer function and its light-fluid approximation: steel plate occupying $\Sigma = -0{\cdot}77\ \mathrm{m} < y < 0{\cdot}77\ \mathrm{m}$, $-0{\cdot}50\ \mathrm{m} < x < 0{\cdot}50\ \mathrm{m}$ in the plane $z = 0$, doubly stiffened with aluminium ribs placed along y-axis at $x = \pm 0{\cdot}17$ m, $z = 0$; source at $y = 0$, $x = -0{\cdot}4$ m, $z = -3$ m; microphones at $y = -0{\cdot}26$ m, $x = -0{\cdot}17$ m, $z = -0{\cdot}25$ m and $y = -0{\cdot}26$ m, $x = -0{\cdot}17$ m, $z = 0{\cdot}25$ m: ––––, light-fluid approximation; ◇–◇–◇–, measured transfer function.

method since the mean third octave analysis, which is of great practical interest, yields differences lower than 3 dB (see Figure 4).

4. CONCLUDING REMARKS

The results presented herein show that the light-fluid approximation provides a suitable tool for acoustic design purposes with rib-stiffened plates surrounded by a gas in the

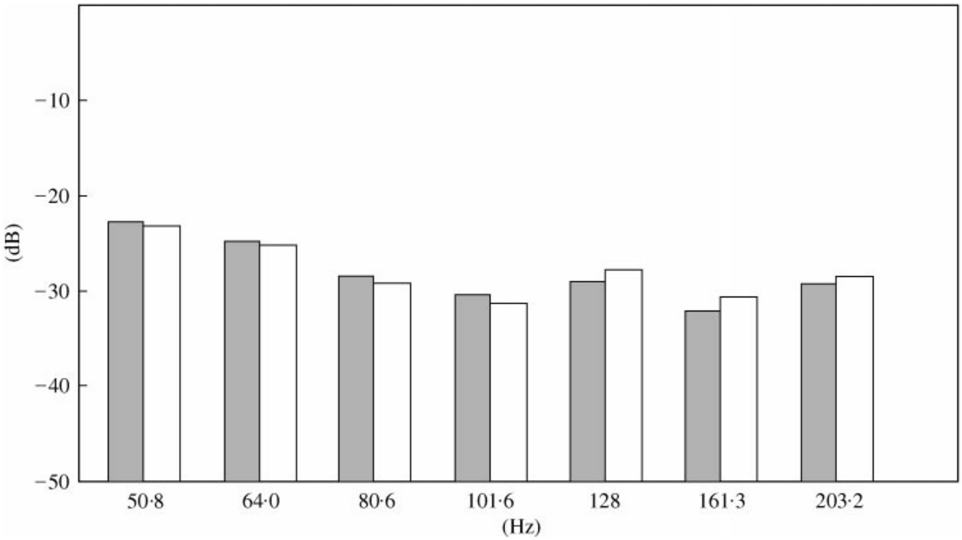

Figure 4. Comparison between the measured mean (third octaves) transfer function and its light-fluid approximation with the same configuration as above: ▦, measured transfer function; □, light-fluid approximation.

low-frequency domain: this is because the *in vacuo* eigenmodes of the structure are rather close to the fluid-loaded structure ones. However, it is necessary to account, even in a first approximation, for the acoustic fluid-loading in order to describe both the radiation damping and the added-mass effects. Indeed, we have checked that the radiation damping of the first 10 eigenmodes is prevailing with respect to the structural damping and therefore cannot be neglected. Furthermore, neglecting the added-mass effect would enable, to a less extent, an overestimation for the real part of the first eigenfrequencies.

For the studied configuration, the perturbation method is numerically efficient since low computational times are required to describe the light fluid-loading effects with a sufficient accuracy. Moreover, the vibro-acoustic problem can also be solved with the same numerical cost up to higher frequencies by a boundary integral equation method for the displacement fields.

REFERENCES

1. B. R. MACE 1981 *Journal of Sound and Vibration* **79**, 439–452. Sound radiation from fluid loaded orthogonally stiffened plates.
2. M. SPIVACK and P. E. BARBONE 1991 *Proceedings of the Royal Society of London* **435**, 615–634. Disorder and localisation in ribbed structures with fluid loading.
3. O. K. BEDAIR 1997 *Journal of Sound and Vibration* **199**, 87–106. Fundamental frequency determination of stiffened plates using sequential quadratic programming.
4. M. MUKHOPADHYAY 1989 *Journal of Sound and Vibration* **130**, 27–40. Vibration and stability analysis of stiffened plates by semi-analytic finite difference method. Part I: consideration of bending displacement only.
5. A. MUKHERJEE and M. MUKHOPADHYAY 1986 *Aeronautical Journal* **120**, 267–273. Finite element free vibration analysis of eccentrically stiffened plates.
6. R. S. LANGLEY 1992 *Journal of Sound and Vibration* **156**, 521–540. A dynamic stiffness technique for the vibration analysis of stiffened shell structures.
7. U. ORRENIUS and S. FINNVEDEN 1996 *Journal of Sound and Vibration* **198**, 203–224. Calculation of wave propagation in rib-stiffened plate structures.

8. D. Habault and P. J. T. Filippi 1998 *Journal of Sound and Vibration* **213**, 333–374. Light fluid approximation for sound radiation and diffraction by thin elastic plates.
9. P. J. T. Filippi, P.-O. Mattei, C. Maury, A. H. P. van der Burgh and G. J. M. de Jong 2000 *Journal of Sound and Vibration* **229**, 1157–1169. Sound transmission through a thin baffled plate: validation of a light fluid approximation with numerical and experimental results.
10. M. Petyt 1977 *Journal of Sound and Vibration* **54**, 537–547. Finite strip analysis of flat skin-stringer structures.
11. L. Cremer, M. Heckl and E. E. Ungar 1988 *Structure-borne Sound*. Berlin: Springer-Verlag; second edition, p. 208.